

## Final Technical Report

**Project Title:** The Influence of Radiation on Pit Solution Chemistry as it Pertains to the Transition from Metastable to Stable Pitting in Steels

**Award Number:** DE-FG02-05ER64003

**Period covered** 1/15/2005 – 7/14/2006

**Recipient:** University of Florida  
Chemistry Department  
P.O. Box 117200  
Gainesville, FL 32611

**Principal Investigator:** Prof. Robert Hanrahan  
(352) 392-1441  
[hanrahan@chem.ufl.edu](mailto:hanrahan@chem.ufl.edu)

**In collaboration with:** Dr. R. Scott Lillard  
Los Alamos National Laboratory  
LANL MS G755  
P.O. Box 1663  
Los Alamos, MN 87545-1663

**Project Team:** Dr. Barbara Galuszka-Muga

## NOTICE

**1. Acknowledgment:** This report was prepared as a result of work supported by the Office of Science (BER), U.S. Department of Energy, Grant No. DE-FG02-05ER64003.

**2. Disclaimer:** Any opinion, findings, and conclusions or recommendations expressed in this material are those of the authors and do not necessarily reflect the views of the Department of Energy.

## Abstract

Previous work relevant to current efforts is summarized. A description of an improved version of a new electrochemical probe, the ArtPit, is given. The distinct feature of the probe for investigating metastable pitting of carbon steels is specified and compared to other approaches. The electrochemical response of the ArtPit under the gamma irradiation and elevated temperature conditions that occur at high level waste (HLW) storage tanks is presented. In particular, the Tafel slope determinations and chemical analyses of the ArtPit confined volume electrolyte are described. Based on results a possible approach for reducing the corrosion rate of HLW tank walls is suggested. Additional statistical analysis of the occurrence of short duration (passivated pits) and long term (stable pitting) electrochemical pulses (current surges) during exposure confirm that radiation enhances the occurrence of both more and smaller sized pits due to increased likelihood of repassivation.

## Objective

The goal of the UF corrosion project is to investigate the effect of high dose levels of gamma radiation on the corrosion mechanism of carbon steels under conditions as similar as possible to those existing at high level waste (HLW) deposits in the US. The approach consists of quantitative electrochemical measurements coupled with chemical analyses of the changing metastable pit environment during irradiation of carbon steel (A516gr70) samples with a 1.0 Mrad/hr (10 kGy/hr) Co-60 gamma source.

## History of Project

Key to the implementation of this project was the adaptation of the UF Co-60 irradiator for *in situ* electrochemical measurements. This facility contains approximately 600 Ci of Co-60 and is capable of generating a nominal 1.25 MeV gamma ray flux of up to 1 Mrad/hour depending on sample position. During the course of this project considerable innovation has been required to meet the challenges of design, development, fabrication, adaptation, reliability, calibration and testing of the various components, units and equipment necessary for accurate electrochemical measurements within the confined space of the irradiator. These efforts include the emplacement of an oven capable of maintaining a temperature of 40 °C comparable to that observed in HLW tanks. Considerable effort was expended in the fabrication and calibration of miniature reference electrodes capable of withstanding the extreme radiation fields encountered. A paper<sup>1</sup> describing this latter effort has been published in *Radiation Physics and Chemistry*.

Early experiments conclusively showed that intense gamma irradiation affected the corrosion process as follows:

- (a) Metastable pitting occurs more frequently in a radiation environment.
- (b) Metastable pitting tends to begin at lower applied voltages in a radiation environment.
- (c) A radiation field tends to produce a larger ratio of Short Duration Pulses (SDP, passivating events) to Long Duration Pulses (LDP, stable pitting), suggesting that, in a radiation environment, repassivation is more easily and quickly established even as the pitting initiation rate increases. Note that these general observations pertain to open coupons immersed in bulk electrolyte. These observations are also consistent with earlier reported trends in studies of high temperature irradiated metals used in nuclear reactor construction<sup>2-5</sup>.

These and other more quantitative results were discussed in Final Technical Report, Award No. DE-FG07-01ER63299 covering the period 9/15/01 - 2/28/05 and will be submitted for publication after review by our collaborators at Los Alamos National Laboratory (LANL).

## Current Progress

Inasmuch as radiation decidedly affects the transition from metastable to stable pitting current efforts centered on understanding the nature and characteristics of these metastable pits. Now, the salient feature of metastable pits is the large ratio of interior pit surface to confined pit electrolyte volume,  $S/V|_{\text{pit}}$  as compared to the ratio,  $S/V|_{\text{bulk}}$  of normal surface area to bulk electrolyte solution to which the sample coupon (in open configuration) is usually exposed. In order to investigate the effect of this confined volume on the pitting mechanism, a device which simulates these pit conditions has been designed and fabricated. This device, called an ArtPit, mimics the nascent pit characteristics insofar as possible and allows the measurement of electrical currents/pulses and more importantly, the analysis of chemical changes which occur in the confined volume due to corrosion in a radiation field and at elevated temperatures. A brief description of an early version of the ArtPit is covered in above mentioned Final Technical Report.

Most often, the usual artificial pit configuration used by prior investigators is that of "lead in pencil"<sup>6</sup>, in which a metal wire or rod is incased in an insulating medium and electrochemically etched to form a pit-like cavity above the exposed metal tip. In rarer cases it consists of simply drilling a small diameter hole to a predetermined depth in the metal of interest<sup>7</sup>. In particular the new configuration better simulates the salient distinction of a real metastable pit, namely the large ratio of interior pit surface to interior pit volume,  $S/V|_{\text{pit}}$ . A comparison of this important ratio for several natural and artificial configurations is shown in Table 1. Clearly the ArtPit configuration most closely resembles the conditions of a real (natural) corrosion pit. Beyond this feature, however, the ArtPit lends itself to the recovery of the confined volume for quantitative analysis of the chemical composition, a feature not possible with other configurations. Moreover the electrical pathway or channel by which the cavity is connected to the bulk electrolyte can be constricted to any desired degree to simulate the rupture of or to control the electrolyte penetration of a passivating film thereby permitting the investigation of this important factor in pit growth.

Table 1. Typical  $S/V$  ( $\text{cm}^{-1}$ ) values or range for pit configurations.

Pit shape or configuration	Typical $S/V$ value or range ( $\text{cm}^{-1}$ )	Typical enclosed volume (mL)
Metastable pit (well-shape) <sup>a</sup>	15,000	$1.7 \times 10^{-11}$
Metastable pit (crevice like) <sup>b</sup>	5,000	$4.0 \times 10^{-6}$
ArtPit	$\sim 100 - 1000^c$	$\sim 0.3 - 3.0 \times 10^{-4}^d$
Lead in pencil <sup>e</sup>	20	$1.0 \times 10^{-4}$
Open coupon <sup>f</sup>	0.006	50.0

<sup>a</sup> hemispherical shape with depth and radius of  $2.0 \times 10^{-4}$  cm ( $2.0 \times 10^4$  Å)

<sup>b</sup> two sided 0.1 cm x 0.1 cm square faces with  $4 \times 10^{-4}$  cm gap between

<sup>c</sup>  $S/V$  ratio determined by thickness of masking layers

<sup>d</sup>  $V$  determined by exposed area and thickness of masking layers

<sup>e</sup> insulated cylindrical cavity with diameter 0.05 cm and depth 0.05 cm

<sup>f</sup> exposed masked area of  $0.3 \text{ cm}^2$  immersed in 50 mL electrolyte

At HLW sites corrosion occurs under conditions of high levels of radiation. No one has to our knowledge explored the chemistry of pit-like electrolytes under irradiation, perhaps

because the experiments and techniques required are tedious, difficult and very time consuming. Moreover, the stochastic nature of the pitting process requires multiple sampling in order to arrive at acceptable mean results for a given set of measurements. Finally these investigations were made at the elevated temperatures  $\sim 40$  °C found in HLW tank contents.

### Methods and Research Approach

During the past year the ArtPit has undergone several modifications as we have refined the design following exploratory experiments. Modification/changes have been made in both the design/fabrication of the ArtPit as well as the protocol for chemical analysis of the confined and limited electrolyte volume (2-4 micro-liters) following disassembly of the ArtPit at the end of each experiment.

A drawing indicating size and assembly of the simulation pit electrode is shown in Fig. 1 and a front view, after assembly, is shown in Fig. 2. It consists of a metal (carbon steel) coupon with attached electrical lead embedded in a hemi-cylindrical epoxy casting. After grinding, polishing and cleaning, the exposed metal surface is masked with electroplating tape so as to define an exposed surface area. A second masking layer, similar to the first layer but with a channel/slit at lower end is placed on top of first layer. After placing a drop of electrolyte on exposed area, the volume is sealed off with a complementary hemi-cylindrical epoxy blank thus trapping the electrolyte within. The assembly is clamped with Teflon rings. In practice the ArtPit serves as the working electrode together with a Pt wire counter electrode and a miniature saturated calomel reference electrode<sup>1</sup> in a 3-electrode electrolysis cell.

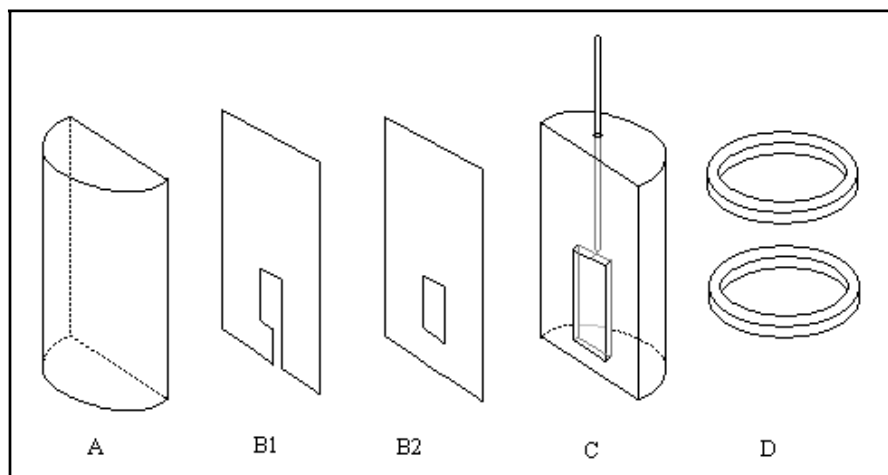


Fig. 1. “Artificial Pit” assembly: slit dimension approximately  $0.3 \text{ cm}^2$ , electroplating tape thickness is  $0.0057 \text{ cm}$ .

A – plastic hemi-cylindrical cover; B1, B2 – electroplating tape with lower slit applied to coupon; C – plastic hemi-cylinder (3 cm length x 0.9 cm diameter) with embedded coupon (2 cm x 0.4 cm x 0.1 cm) and insulated electrical wire attachment through top; D – Teflon rings for clamping hemi-cylinders together.

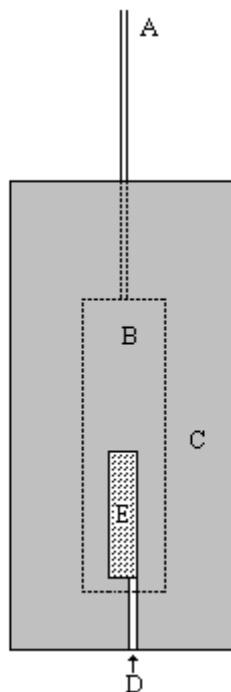


Fig. 2. Front view of working “Artificial Pit” electrode. Coupon embedded in hemi-cylindrical epoxy mold with electroplating tape overlay (dark portion) showing slit and exposed (dotted area) coupon area.

A - electrical wire attachment; B - embedded coupon; C - corrosion tape overlay/ mask; D - electrolyte solution access channel; E - exposed coupon area (dotted area).

The chemistry composition of the ArtPit volume is determined by ion chromatography (Dionex IC) to detect and quantify the presence of metal ions ( $\text{Fe}^{2+}$ ,  $\text{Fe}^{3+}$ , and  $\text{Mn}^{2+}$ ) resulting from the corrosion induced dissolution of the carbon steel. Parallel samples are run in order to average out the stochastic nature of the initiation of the pitting process even under controlled conditions. As stated above the primary objective remains that of measuring the effect, both electrical and chemical, on the pitting of a limited (confined) electrolyte volume at the carbon steel surface with and without radiation at 40 °C.

Concurrent with these chemical composition analyses, we have explored the effect of radiation on the stability (with respect to corrosion) of the metal surface. The "Tafel slope"<sup>8,9</sup> shifts of ArtPit surfaces indicate that an irradiation environment raises the corrosion potential ( $E_{\text{corr}}$ ) or open circuit potential (OCP) suggesting an increased resistance to pitting in the ArtPit. The higher the value of OCP, the more resistant the coupon surface is to corrosion *via* the pitting process.

## Results

*Use of "Tafel slope"<sup>8,9</sup> to measure offset/displacement of  $E_{\text{corr}}$ .*

The objective of these experiments is to record the log of current density vs. IR corrected potential in order to compare the offset of the "Tafel slopes" generated by gamma irradiation. For example, Newman<sup>10</sup> has determined that the corrosion inhibiting effect of 2.7% by weight molybdenum (Mo) in Fe-Cr-Ni steels is measured by an offset (increase) of the "Tafel slope" by

60 mV and an accompanying increase of about 130 mV in the corrosion potential  $E_{\text{corr}}$  of the pit solution. In a similar manner we use the "Tafel slope" offset to interpret the effect of ionizing radiation on the corrosion potential generated in the ArtPit confined electrolyte.

In a typical setup, an applied potential (AP) between a Pt mesh counter electrode and an ArtPit working electrode is monitored by a miniature saturated calomel electrode (MSCE). After stabilizing for one hour at OCP (zero AP), the current density is recorded as a stepwise potentiostatic (PS) application. The AP is begun about 0.4 V above OCP and is decreased in 0.020 V steps until minimum current is reached. Experiments were run in pairs, with and without irradiation, in 1.0 M NaCl electrolyte solution at 40 °C. Typical plots are shown in Fig. 3. From these plots an estimate of the solution resistance ( $R_{\text{soln}}$ ) was made by extrapolating the slope at smallest current values. Using this value the IR correction was made for each data point according to the relation:

$$AP_{\text{calc}} = AP_{\text{expt}} - IR_{\text{soln}}$$

where  $AP_{\text{calc}}$  is the corrected value of applied voltage,  $AP_{\text{expt}}$  is the experimentally applied potential across the cell,  $I$  is the measured current in amps and  $R_{\text{soln}}$  is taken in ohms [note:  $I(\text{amps}) = I_{\text{density}}(\text{amps/cm}^2) \times A(\text{cm}^2)$ , where  $A$  = exposed coupon surface area]. The resulting nearly straight line approximated the corrected Tafel slope. Refinement of this slope was made by adjusting the value of  $R_{\text{soln}}$  about the estimated value until the best straight line fit was obtained as shown in Fig. 4. Tafel slope data were acquired under two different procedures of corrosive conditions, in paired samples either without irradiation or exposed to ~1Mrad/hour of Co-60 gamma rays. In the first group a potentiodynamic (PD) scan followed the initial stabilizing 1 hour open circuit potential (OCP) step and preceded the Tafel slope determination. The PD step ended at 0.0 V (*re* MSCE) before beginning the third step. During the Tafel slope determination the applied potential (AP) beginning at 0.0 V (*re* MSCE) was cycled, after each incremental lower step to acquire a data point, back up to the starting point of 0.0 V (*re* MSCE). Data from three pair of ArtPit configured coupons was collected in this mode and showed a uniform offset of the Tafel slope under irradiation conditions to more positive potentials, up to ~20 mV, indicating an unexpected lower current density and a lesser rate of corrosion. In the second group of six pair of electrodes, no PD scan was inserted between the opening OCP step and the Tafel slope determination. The latter began at an AP of 0.0 V (two pair) or -0.3 V (four pair) stepping down (as done for first group) by 0.020 V increments before recycling back to beginning voltage, and proceeded until a minimum current was reached. For this group of ArtPits the Tafel slope positions, with and without irradiation exposure, varied considerably as evidenced from data collected from six pair of coupons. Tafel slope offsets were both positive and negative when compared to the no radiation conditions, indeed considerable offset variation occurred within each category, *i.e.* with and without radiation exposure, though slightly more so for those coupons exposed to gamma radiation. The interpretation is that stabilizing of the ArtPit coupon surface has not yet occurred or that possibly gas pockets occur within the ArtPit confined volume, thus affecting the apparent solution resistance and/or potential drop across the surface. Examples of this variation are shown in Fig. 5 (for no radiation) and 6 (with gamma irradiation). Clearly, it is desirable to acquire more reproducible configurations and conditions in order to gain more insight into the effect of radiation on the Tafel slope approach and its relation to corrosion dynamics.

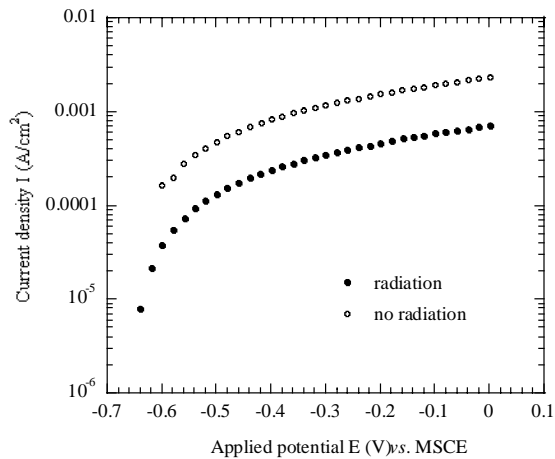


Fig. 3. Current density vs. applied potential for ArtPit with radiation and without radiation.

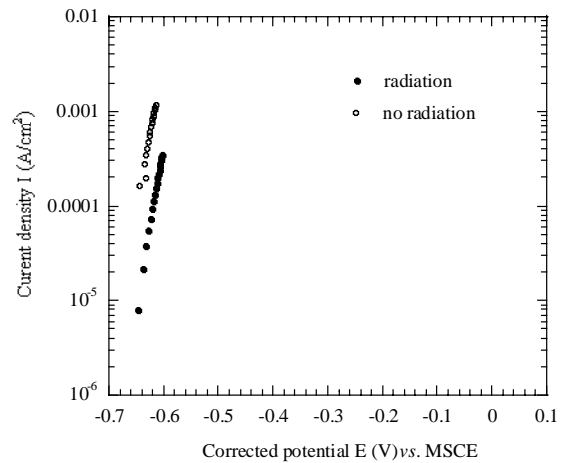


Fig. 4. Current density vs. IR corrected applied potential for ArtPit with radiation and without radiation.

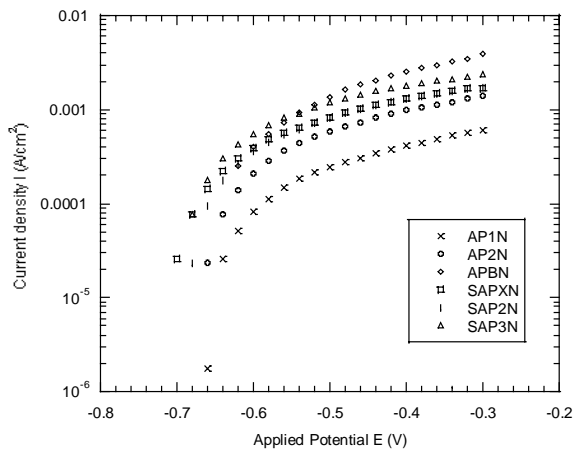


Fig. 5. Tafel slope progression for non-irradiated ArtPits.

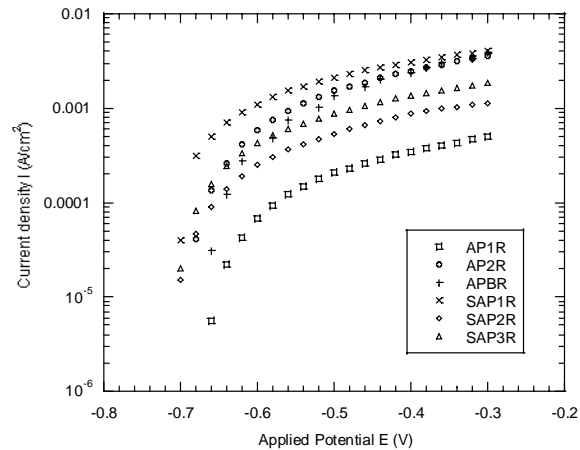


Fig. 6. Tafel slope progression for irradiated ArtPits.

#### Chemical Analyses - Enlarged $Fe^{2+}/Fe^{3+}$ Ratio, $Fe^{2+,3+}/Mn^{2+}$ Ratio.

The chemical analysis of the pit solution is the most direct way of determining the chemical change which occurs due to corrosion. We have developed procedures for determining  $Fe^{2+}$ ,  $Fe^{3+}$  and  $Mn^{2+}$  content in the confined volume (2 - 4 microliters) of the ArtPit. Generally, after a corrosion experiment [(a) one hour OCP exposure followed by Tafel slope determination, or (b) only a one hour corrosion induced at OCP, (all at 40 °C in 1 M NaCl electrolyte)] the ArtPit is rinsed, dried with Kimwipes and carefully disassembled over a tared weighing bottle. The adherent electrolyte from the confined volume is washed and recovered using a spitzer attached to micro-syringe (a very delicate task). To the rinsed-off volume is added one drop of 0.40 M  $H_2SO_4$  to stabilize any  $Fe^{2+}$  therein. The amount of recovered volume is determined by weighing and converting using a density factor of 1.0 g/mL. A hundred  $\lambda$  of this rinse solution is further diluted with 1 mL DI water (11:1 dilution). Each of these solutions (0.5 to 1.1 mL) is



used in a single analysis by injection into a 0.100 mL (100  $\lambda$ ) sample loop in an ion chromatograph (Dionex IC) unit which has been calibrated for quantitative determination of  $\text{Fe}^{3+}$ ,  $\text{Cu}^{2+}$ ,  $\text{Ni}^{2+}$ ,  $\text{Zn}^{2+}$ ,  $\text{Mn}^{2+}$  and  $\text{Fe}^{2+}$  ions, eluted in that order. Fig. 7 represents a typical elution plot and Figs. 8 - 10 show calibration curves for  $\text{Fe}^{3+}$ ,  $\text{Mn}^{2+}$  and  $\text{Fe}^{2+}$ . Fig. 11 is an elution curve from an ArtPit rinse solution showing the actual peak areas from an exploratory run. Calculations are then made to determine the molar concentrations, total weight of ions and appropriate ion ratios in the original ArtPit volume.

The view which emerges is tentatively as follows:

- (a) For ArtPits undergoing a sequence of 1 hour OCP, PD ending at 0.0 V AP, potentiostatic (PS) Tafel slope determination, a single paired sample resulted in  $\text{Fe}^{2+}/\text{Fe}^{3+}$  ratios of 26/1 and 147/1 for non-radiation and irradiation conditions, respectively.
- (b) For ArtPits undergoing a sequence of 1 hour OCP followed by PS Tafel slope determination:
  - (1) The  $\text{Fe}^{2+}/\text{Fe}^{3+}$  ratio for both irradiation and non-radiation conditions was generally higher when Tafel slope was offset to more positive voltages concurrently with lower recorded currents.
  - (2) The  $\text{Fe}^{2+}/\text{Fe}^{3+}$  ratios for both irradiated and non-irradiated samples varied considerably from a low of 3/1 to a high of 86/1. No statistically significant difference in response between the two sets was established.
  - (3) The ratio of  $\text{Fe}^{2+}$  in non-irradiated samples to that in irradiated samples,  $\text{Fe}^{2+}(\text{N}) / \text{Fe}^{2+}(\text{R})$  was greater than 1/1 consistent with the interpretation that more corrosion occurred in the former (non-irradiated) samples under nearly identical conditions (other than the irradiation). This effect is contrary to the observations for open coupons.
  - (4) The ratio of total  $\text{Fe}^{2+,3+}/\text{Mn}^{2+}$  in all samples was about 200/1. The carbon steel coupon composition weight ratio Fe/Mn is 88.5/1 indicating preference for iron dissolution over that of manganese. An alternate explanation is the failure to recover an insoluble manganese oxide during the rinse recovery step.
- (c) For samples for which only a 1 hour OCP preceded a chemical analysis of the ArtPit confined volume:
  - (1) The  $\text{Fe}^{2+}/\text{Fe}^{3+}$  ratio was 26/1 for non-irradiated and 41/1 for irradiated ArtPits, based on three paired samples, though a large variation occurred within each set.
  - (2) The total  $\text{Fe}^{2+,3+}/\text{Mn}^{2+}$  ratio in two irradiated ArtPit samples averaged over 200/1 indicating substantial deficiency in the dissolution of Mn relative to Fe.
  - (3) A wide variation in OCP values occurred during the 1 hour OCP recording as the confined volume of electrolyte equilibrated to the imposed conditions.

Overall, a wide variation in ArtPit response was observed as the imposed conditions and procedures were activated. Clearly, further experimental investigation of the ArtPit configuration is needed to develop its potential as a valid electrochemical probe.

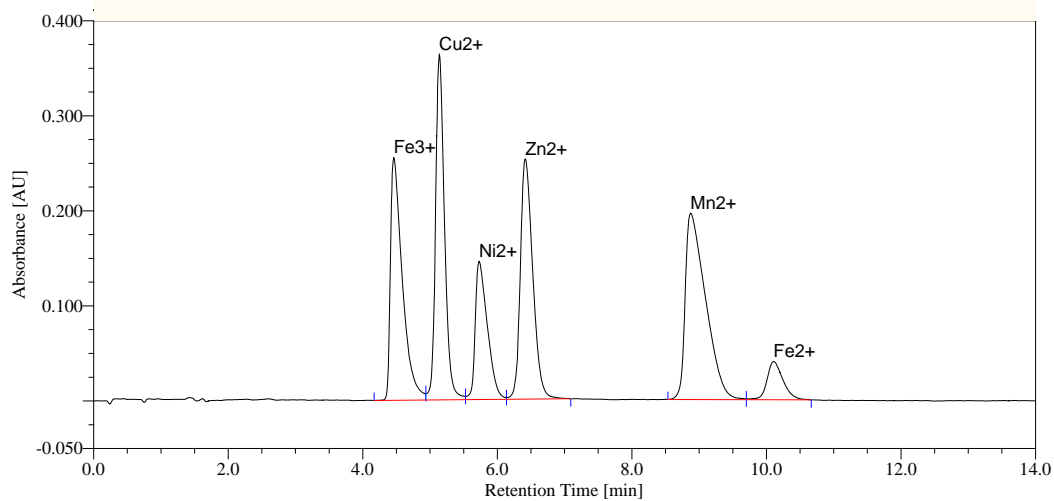


Fig. 7. Chromatogram of a standard solution containing 2.0 ppm of  $\text{Fe}^{3+}$ , 2.0 ppm of  $\text{Cu}^{2+}$ , 6.0 ppm of  $\text{Ni}^{2+}$ , 2.0 ppm of  $\text{Zn}^{2+}$ , 4.0 ppm of  $\text{Mn}^{2+}$  and 2.0 ppm of  $\text{Fe}^{2+}$ .

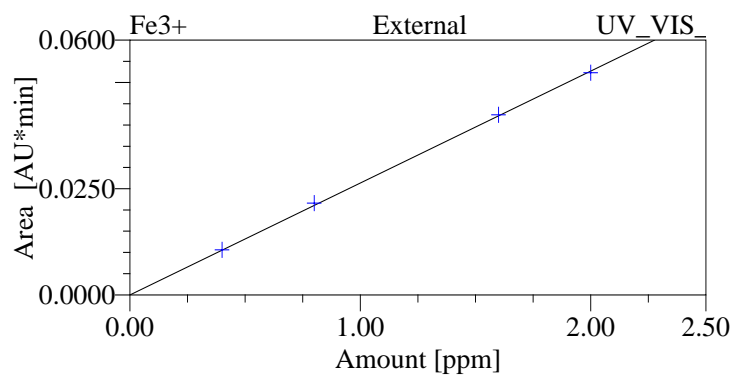


Fig. 8. Calibration curve for  $\text{Fe}^{3+}$  ion.

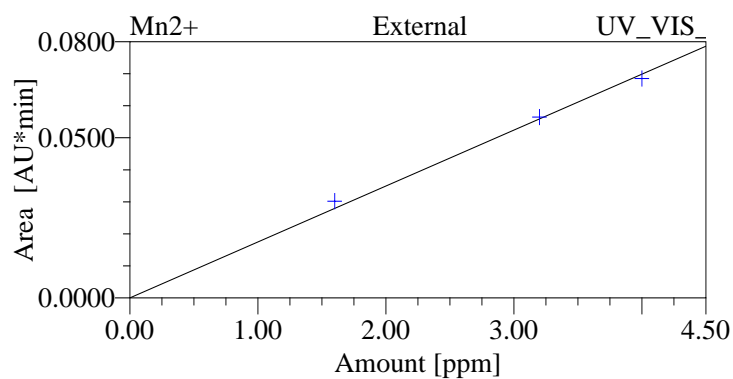


Fig. 9. Calibration curve for  $\text{Mn}^{2+}$  ion.

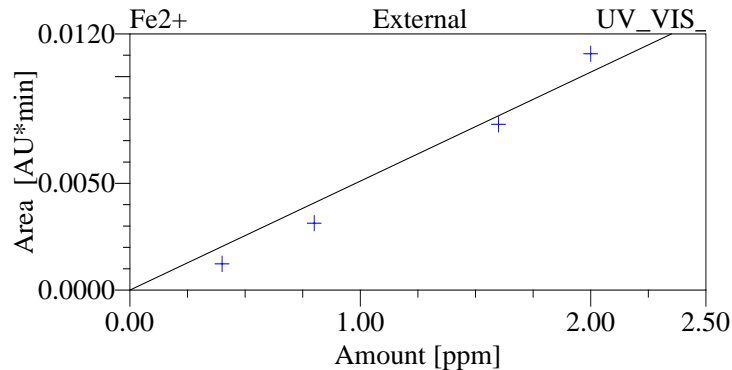


Fig. 10. Calibration curve for  $\text{Fe}^{2+}$  ion.

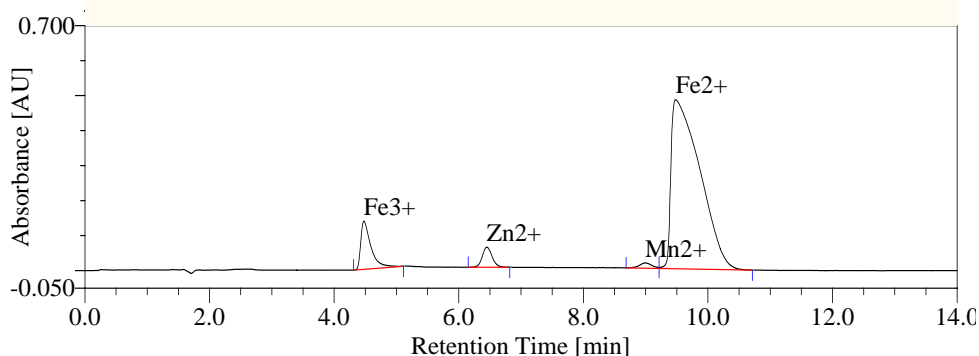


Fig.11. Chromatogram of ArtPit solution.

A surprising result of the chemical analyses is the large ratio of  $\text{Fe}^{2+}/\text{Fe}^{3+}$  found in the ArtPit volume. Normally, one expects (in a radiation field) a rapid conversion of  $\text{Fe}^{2+} \rightarrow \text{Fe}^{3+}$ , indeed this reaction is the basis for the Fricke Dosimetry<sup>11</sup> determination of radiation dose. It is possible that (a) the non-occurrence of this conversion is due to a rapidly attained anoxic condition generated by gamma irradiation or (b) the effect may be a result of the higher ion concentrations developed (*via* disproportionation reactions) in the confined (limited) electrolyte volume thus simulating a passivating pit, or (c) limited intrusion of counter ions (anions) into the constricted volume inhibits further oxidation, or (d) a combination of these factors occurs.

Putting these results together, a consistent picture of ArtPit corrosion begins to emerge, namely, (a) the Tafel slope shift indicates increased resistance to corrosion (possibly from passivation of incipient pits) under irradiation, (b) increased  $\text{Fe}^{2+}/\text{Fe}^{3+}$  ratio indicates a less oxidizing environment in the confined volume causing pit passivation.

In light of the above and as a practical matter, the simple action of (a) displacement (flushing out) of dissolved oxygen by sparging with pure nitrogen gas, (b) addition of  $\text{Fe}^{2+}$  to tank contents, together with (c) the natural irradiation environment from high level wastes, could, while not totally preventing corrosion, significantly retard corrosion in HLW tanks. Essentially, we propose adjusting the bulk electrolyte to mirror the electrolytic environment inside the ArtPit. Since compressed nitrogen is relatively inexpensive, this could be a cost-effective approach to HLW tank corrosion control/retardation. Further studies are required to examine this possibility.

### Additional Measurements - Statistics at Different Applied Potentials

To improve statistical validation, we harvested additional data on the size (*i.e.* charge surge which is related to pit size) and frequency of metastable pitting (with and without irradiation) during potentiostatic (PS) experiments (PS holds of 40 minute duration each) of A516gr70 carbon steel coupons at preset elevated applied potentials (AP) at 40 °C. The electrolyte was 0.11 M NaCl/0.19 M NaOH; applied potentials of 0.00, 0.15, 0.30, 0.38 and 0.42 V vs. MSCE (sat'd. calomel reference electrode). No correlation was observed between pitting frequency and applied potential (AP) over this range; the maximum AP was still below the pitting potential  $E_{pp}$  for these samples. However the cumulative data over all AP's have been plotted as histograms in Figs. 12 and 13. These plots confirm the dominance of the smaller metastable pits (with and without radiation exposure) and the observation that radiation enhances the occurrence of more and smaller sized pits due to increased likelihood of repassivation. These data have been transmitted to our collaborators at Los Alamos National Lab (LANL) for incorporation into an article now in preparation.

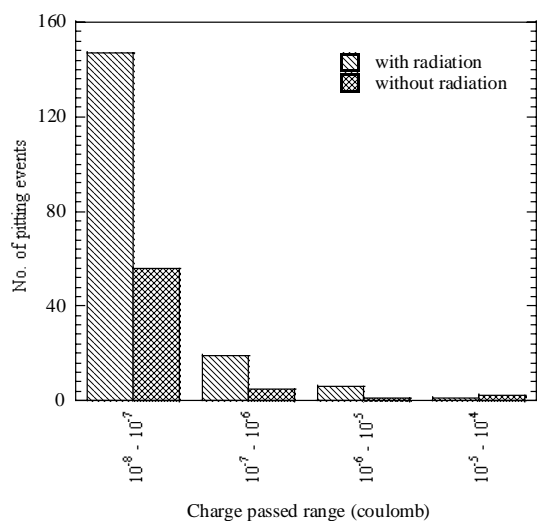


Fig. 12. Histogram of pitting events for six pairs of A516gr70 samples.

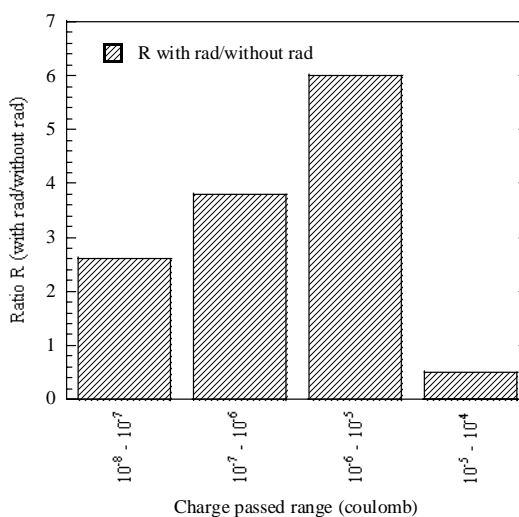


Fig. 13. Histogram of ratio R of pitting events with radiation to number of pitting events without radiation.

### Information Access

1. B. Galuszka-Muga, M.L. Muga, R.J. Hanrahan, M.A. Hill and R.S. Lillard, "The Influence of Gamma Radiation on Pitting Corrosion of Carbon Steels in Alkaline High Level Radioactive Waste Tanks", manuscript in preparation.
2. M.L. Muga, B. Galuszka-Muga "The ArtPit, a Different Artificial Corrosion Pit Configuration", manuscript pending further experimental work development.

### References

1. B. Galuszka-Muga, M.L. Muga, R.J. Hanrahan, *The effect of gamma radiation on the stability of miniature reference electrodes*. Rad. Phys. Chem. **75**, No. 9, pp. 927-931 (2006).
2. B. Cox, *Oxidation of zirconium and its alloys*. Advances in Corrosion Science & Technology, **5**, pp. 173-391 (1976).

3. W. G. Burns and P. B. Moore, *Water radiolysis and its effect upon in-reactor zircaloy corrosion*. Radiation Effects, **30**, pp. 233-242 (1976) and *Radiation enhancement of zircaloy corrosion in boiling water systems: a study simulated radiation chemical kinetics*. Water Chem. Nucl. React. Syst., Proc. Int. Conf. (1978), British Nuclear Energy Society, London 1977, pp. 281-289, 311-313.
4. W. G. Burns, W.R. Marsh and W. S. Walters, *The  $\gamma$  irradiation-enhanced corrosion of stainless and mild steels by water in the presence of air, argon and hydrogen*. Radiation Phys. Chem., **21**, No. 3, pp. 259-279 (1981).
5. N. Fujita, C. Matsuura and K. Saigo, *Irradiation-enhanced corrosion of carbon steel in high temperature water - in view of a cell formation induced by  $\gamma$ -rays*. Radiation Phys. Chem., **58**, pp. 139-147 (2000).
6. R. C. Newman and H. S. Isaacs, *Diffusion-Coupled Active Dissolution in the Localized Corrosion of Stainless Steels*. J. Electrochem. Soc., **130**, pp. 1621-1624 (1983).
7. H. S. Isaacs, *The Behavior of Resistive Layers in the Localized Corrosion of Stainless Steel*. J. Electrochem. Soc., **120**, No. 11, pp. 1456-1462 (1973).
8. J. Tafel, Z. Phys. Chem., **50**, p. 641 (1904).
9. D. A. Jones, "Principles and Prevention of Corrosion", 2nd Ed., Prentice Hall, N.J. ISBN 0-13-359993-0, Chapt. 3, pp. 80-98, 1996.
10. R. C. Newman, *The Dissolution and Passivation Kinetics of Stainless Alloys Containing Molybdenum -II. Dissolution Kinetics in Artificial Pits*. Corrosion Science, **25**, No. 5, pp. 341-350 (1985).
11. H. Fricke and S. Morse, *The Chemical Action of Roentgen Rays on Dilute Ferrosulfate Solutions as a Measure of Dose*. Am. J. Roentgenol. Radium Ther. Nucl. Med., **18**, pp. 426-430 (1927).

### **Acknowledgments**

The authors would like to thank the Office of Science, U.S. DOE for its financial support of this project. We would like to acknowledge the volunteer contribution of Dr. Luis Muga, Prof. Emeritus, UF, who, with Dr. Barbara Galuszka-Muga, originated, developed and tested the ArtPit concept reported herein. Also we thank Mary Ann Hill of Los Alamos National Laboratory for help in setting up the CorrWare/CorrView control of electrochemical experiments.